A Millimeter-Wave Six-Port Reflectometer Using Dielectric Waveguide

GEORGE HJIPIERIS, MEMBER, IEEE, RICHARD J. COLLIER, AND ERIC J. GRIFFIN

Abstract—**A novel six-port reflectometer circuit is described which is particularly suited to dielectric-type waveguides. Its scattering matrix is derived allowing for flexibility in design. A phase shifting network is incorporated in the circuit and it is shown that a quadrature hybrid can be configured for this purpose. The reflectometer is implemented in dielectric waveguide for *W*-band (75 GHz–110 GHz) operation and measurements are presented.**

I. Introduction

DIELECTRIC-TYPE waveguides have emerged as viable alternatives to rectangular waveguide and finline at millimeter wavelengths. They are generally low-loss transmission lines [1], have large usable bandwidths [2], and are easy to fabricate at low cost. Some, such as image guide [3] and nonradiative dielectric guide [4], utilize ground planes which, apart from improving electrical performance, also provide support for the dielectric and allow device mounting [5]. They are, however, all variants of dielectric waveguide, which is simply a dielectric rod of uniform rectangular cross section. Various methods have been proposed for the analysis of dielectric waveguide [6]–[9], some of which involve large-scale computation, but they all predict similar behavior over the operational bandwidth. A large variety of components for use with dielectric-type waveguides have also been investigated [10]–[12], and their designs are readily available in the open literature.

The six-port technique for measuring complex reflection coefficient, originally developed by Engen and Hoer [13]–[15], is now well established in the microwave art. Vector information is computed from scalar measurements of power with comparable, if not better, accuracy to the other measurement techniques [16], [17] and often at lower cost. To date a large number of six-port circuits have been described but not all are suitable for implementation in dielectric waveguide. Some circuits utilize specialized components [18], [19] which as yet have no direct equivalents in dielectric waveguide, while others [21] exclude the use of available components due to the resulting nonplanar topology. The six-port circuit described in this paper removes the aforementioned restrictions, and the results obtained with its dielectric waveguide implementation demonstrate the viability of the latter as a transmission medium suitable for multicomponent integration.

Manuscript received August 13, 1987; revised August 15, 1989. The work described in this paper formed part of the doctoral dissertation of G. Hjipieris and was supported by the Department of Industry under Contract RD 207-01.

G. Hjipieris was with the Electronic Engineering Laboratories, University of Kent, Canterbury, U.K. He is now with Marconi Instruments, Stevenage, U.K.

R. J. Collier is with the Electronic Engineering Laboratories, University of Kent, Canterbury, U.K.

E. J. Griffin is with R.S.R.E., Malvern, U.K.

IEEE Log Number 8931557.

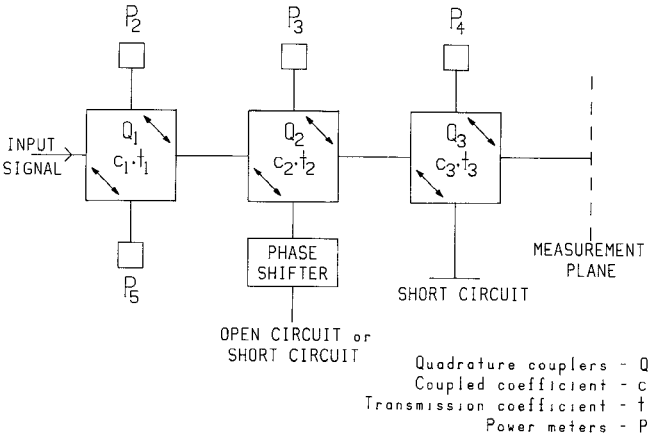

Fig. 1. Proposed six-port circuit.

II. Circuit Description

The proposed circuit [22], [23] is depicted in its most general form in Fig. 1. It consists of three quadrature couplers, a phase shifter, a short circuit, and an open circuit together with the connecting lengths of transmission line. The open circuit is readily replaced with a short circuit for transmission media, such as rectangular waveguide and finline, where broad-band open circuits cannot be realized. Alternatively, as will be shown in Section V, a quadrature coupler can perform the same function as the phase shifter and open circuit combination.

Some of the attractive features of this circuit as follows.

a) There are no "cross-overs," which results in a planar topology. Thus it can be implemented in any guiding medium and also lends itself to integration.
b) The quadrature couplers are arranged in a serial fashion and therefore any type of quadrature coupler can be used.
c) If a quadrature coupler is used to realize the phase shifter and open circuit, then the circuit's performance is independent of any inequality in phase

0018-9480/90/0100-0054$01.00

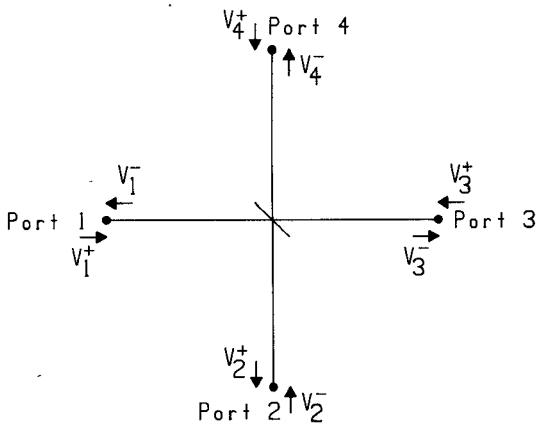

Fig. 2. Quadrature coupler with wave labeling.

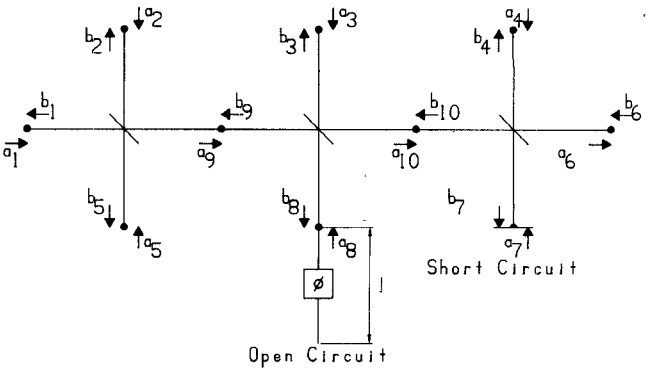

Fig. 3. Six-port circuit with wave labeling.

velocity in the couplers and connecting transmission lines. This is because all waves incident at any detector port have traveled through an equal number of identical couplers and lines.

d) The circuit can be constructed from readily available "off-the-shelf" components in standard transmission lines.

III. Circuit Analysis

The equations governing the performance of any six-port reflectometer can be derived from the circuit's scattering coefficients. In order to obtain the scattering matrix of the proposed circuit, the properties of the four-port couplers must first be qualified. For the ideal quadrature coupler shown in Fig. 2, where the dots represent the accessible ports, the ingoing, V_n^+, and outgoing, V_n^-, waves are related for the given port numbering by

$$\begin{bmatrix} V_1^- \\ V_2^- \\ V_3^- \\ V_4^- \end{bmatrix} = \begin{bmatrix} 0 & jn & m & 0 \\ jn & 0 & 0 & m \\ m & 0 & 0 & jn \\ 0 & m & jn & 0 \end{bmatrix} \begin{bmatrix} V_1^+ \\ V_2^+ \\ V_3^+ \\ V_4^+ \end{bmatrix} \tag{1a}$$

where

$$n = N\exp(-j\theta)$$
$$m = M\exp(-j\theta). \tag{1b}$$

N and M are the amplitude coefficients and θ is the phase change due to the physical separation between any two ports, assumed to be identical. If the coupler is lossless then

$$N^2 + M^2 = 1.$$

Fig. 3 shows the six-port circuit with wave labeling to aid the analysis. It is assumed that all connections take place at the accessible ports of the couplers and l is the electrical length between the open circuit and coupler port.

The outgoing waves at the six ports, $b_{1\ldots6}$, can be expressed in terms of the ingoing waves, $a_{1\ldots6}$, by expanding (1) as applied to the circuits couplers and using

$$a_7 = -b_7 \tag{2}$$

$$a_8 = b_8 \exp 2j(-\theta_l + \phi) \tag{3}$$

where θ is the phase change in an electrical length, l, and ϕ is the phase change due to the phase shifter.

The resulting scattering matrix $[S_6]$ is described by the following equation:

$$[S_6] = \begin{bmatrix} m^2m^2n^2 - m^2n^2\exp^{2j(-\theta_l+\phi)} & jn_1m_1m_2n_3 - jn_1m_1n_2\exp^{2j(-\theta_l+\phi)} & jm_1m_2n_2n_3 + jm_1m_2n_2\exp^{2j(-\theta_l+\phi)} & -jm_1m_2m_3n_3 & jn_1 & m_1m_2m_3 \\ jn_1m_1m_2n_3 - jn_1m_1n_2\exp^{2j(-\theta_l+\phi)} & -n^2m^2n^2 + n^2n^2\exp^{2j(-\theta_l+\phi)} & -n_1n_2m_2n_3 - n_1m_2n_2\exp^{2j(-\theta_l+\phi)} & n_1m_2m_3n_3 & m_1 & jn_1m_2m_3 \\ jm_1n_2m_2n_3 + jm_1n_2m_2\exp^{2j(-\theta_l+\phi)} & -jm_1m_2n_3m_3 & S - n_2n_3 + m_2\exp^{2j(-\theta_l+\phi)} & n_2n_3m_3 & 0 & jn_2m_3 \\ jn_1 & m_1 & n_2n_3m_3 & -m_3 & 0 & jn_3 \\ m_1m_2m_3 & jn_1m_2m_3 & 0 & 0 & 0 & 0 \\ & & Sjn_2m_3 & jn_3 & 0 & 0 \end{bmatrix} \tag{4}$$

$[S_6]$ can now be used to obtain the responses at ports 2, 3, 4, 5 to an input signal at port 1, V_0, with a device under test (DUT) having a reflection coefficient Γ at port 6. If the sensors used to detect the responses, and together with the source, are assumed to be matched to the circuit, then

$$\begin{bmatrix} b_1 \\ b_2 \\ b_3 \\ b_4 \\ b_5 \\ b_6 \end{bmatrix} = [S_6] \begin{bmatrix} V_0 \\ 0 \\ 0 \\ 0 \\ 0 \\ \Gamma b_6 \end{bmatrix}$$

The detectors, whether diodes or of the thermistor type, are square law devices and their indications $P_{2,3,4,5}$ are proportional to |voltage|^2. For identical detectors,

$$\frac{P_2}{P_5} = \left|\frac{b_2}{b_5}\right|^2 = M_1^2 M_2^4 M_3^4 \left|\Gamma + \frac{N_3^2}{M_3^2} - \frac{N_2^2 \exp 2j(-\theta_l + \phi)}{M_2^2 M_3^2 \exp(-2j\theta)}\right|^2 \tag{5a}$$

$$\frac{P_3}{P_5} = \left|\frac{b_3}{b_5}\right|^2 = \frac{N_2^2}{N_1^2} M_1^2 M_2^2 M_3^2 \left|\Gamma \frac{N_3^2}{M_1^2} + \frac{\exp 2j(-\theta_l + \phi)}{M_3^2 \exp(-2j\theta)}\right|^2 \tag{5b}$$

$$\frac{P_4}{P_5} = \left|\frac{b_4}{b_5}\right|^2 = \frac{N_3^2}{N_1^2} M_1^2 M_2^2 M_3^2 |\Gamma - 1|^2 \tag{5c}$$

where (1b) has been used to distinguish between the amplitude and phase terms of the coupling coefficients. For nondispersive components these power ratios can be made frequency independent by ensuring that $\theta_l = \theta$.

Equation (5) describes three circles, often called impedance locating circles, in the complex Γ plane. At a given frequency their centers are fixed, the positions being determined by the circuit's scattering coefficients, while their radii are proportional to the square root of the power ratios. Every point in the Γ plane has a unique combination of power ratios associated with it, and in geometrical terms this corresponds to the three impedance locating circles intersecting in one point—the reflection coefficient of the DUT.

It should be noted that the formulation of six-port operation presented here is a special case of the general bilinear relationship which exists between the power ratios and Γ. The simplification arises from the assumptions of perfect coupler isolation and matched source and detectors. With reference to the proposed circuit, this is equivalent to P_5 being independent of the DUT. Had these assumptions not been made, then the design, which consists of positioning the impedance locating circles, would become quite complicated as the six-port scattering matrix would need to be inverted.

IV. Design

The positions of the impedance locating circle centers depend on the choice of coupling coefficients and phase shift in (5a)–(5c). An easily realizable phase shift is $2\phi = \pi/2$ (Section V), and this results in

$$\frac{P_2}{P_5} = M_1^2 M_2^4 M_3^4 \left|\Gamma + \frac{N_3^2}{M_3^2} - \frac{jN_2^2}{M_2^2 M_3^2}\right|^2 \tag{6a}$$

$$\frac{P_3}{P_5} = \frac{N_2^2}{N_1^2} M_1^2 M_2^2 M_3^2 \left|\Gamma + \frac{N_3^2}{M_3^2} + \frac{j}{M_3^2}\right|^2 \tag{6b}$$

$$\frac{P_4}{P_5} = \frac{N_3^2}{N_1^2} M^2 M^2 M^2 |\Gamma - 1|^2. \tag{6c}$$

For 3 dB couplers the performance equations thus become

$$\frac{P_2}{P_5} = \frac{1}{32}|\Gamma + 1 - 2j|^2 \tag{7a}$$

$$\frac{P_3}{P_5} = \frac{1}{16}|\Gamma + 1 + 2j|^2 \tag{7b}$$

$$\frac{P_4}{P_5} = \frac{1}{8}|\Gamma - 1|^2 \tag{7c}$$

with the impedance locating circles centered at

$$(-1, 2)$$
$$(-1, -2)$$
$$(1, 0).$$

Engen [15] notes that ideally the centers should be symmetrically distributed at 120° intervals around the origin. This circuit nearly achieves this target with angles of 116.57°, 116.57°, 126.87° although the power ratios for a matched load are unequal.

V. Phase Shifting Network

The six-port circuit described in the preceding sections requires a reciprocal $\pi/4$ phase shifter terminated in an open circuit such that the overall phase shift is $\pi/2 - 2\theta$, where θ is the phase delay due to propagation between two ports of a quadrature coupler.

A method of achieving the desired phase shift over a broad band is presented, which employs a quadrature coupler. This technique also reduces the number of different components necessary for the six-port circuit to 2, quadrature couplers and a short circuit. Consider the coupler configuration and wave labeling of Fig. 4. The coupled and through ports are connected together, with the isolated port terminated in a matched load. If n is the coupling coefficient and m the transmission coefficient, then using (1) and

$$V_3^- = V_2^+$$
$$V_2^- = V_3^+$$

gives

$$V_1^- = 2NMV_1^+ \exp j(\pi/2 - 2\theta) \tag{8}$$

$$V_4^- = (M^2 - N^2)V_1^+ \exp(-j2\theta). \tag{9}$$

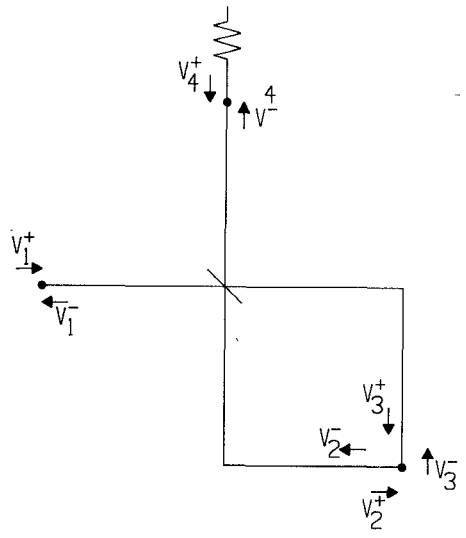

Fig. 4. Phase shifting network using quadrature hybrid.

If $M^2 = N^2 = 1/2$, then

$$V_1^- = V_1^+ \exp j(\pi/2 - 2\theta)$$
$$V_4^- = 0$$

and the desired phase shift has been achieved with no loss of power in the matched load. Any deviation from quadrature by the coupler is represented by the term following $\pi/2$ in (8).

In practice, coupler ports cannot generally be directly connected and therefore an extra length of transmission line is necessary. If the length is L and the associated phase delay δ_L, then

$$V_1^- = V_1^+ \exp j(\pi/2 - 2\theta - \delta_L) \qquad (10)$$

and this length must be compensated for in the six-port circuit by offsetting both the DUT and the short circuit by a length $1/2\ L$.

The phase shifting network was assembled in X-band (8.5–12 GHz) rectangular waveguide because of the availability of phase measuring facilities. An indirect method of verifying (10) was adopted which consisted of the following steps:

a) The coupler was characterized by measuring the phase responses ϕ_c and ϕ_t at the coupled and through ports together with the amplitude response. The phase difference $\phi_c - \phi_t$ was determined using a storage normalizer.

b) The phase response, ϕ_{ps}, of the network (Fig. 5(a)), with the coupled and through ports connected together using two equal lengths of flexible guide, was measured. Ideally

$$\phi_{ps} = \phi_c - \phi_t - 2\theta - \delta_L.$$

c) The coupled port was terminated in a matched load and the single length of flexible waveguide was connected to the through port and short-circuited as in Fig. 5(b) while still retaining the same curvature as in step (b) and the phase response, ϕ_{sc}, measured:

$$\phi_{sc} = -2\theta - \delta_L - \pi.$$

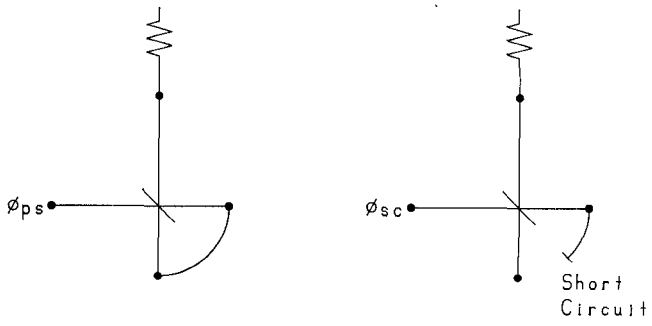

Fig. 5. Determination of phase shifter's phase response.

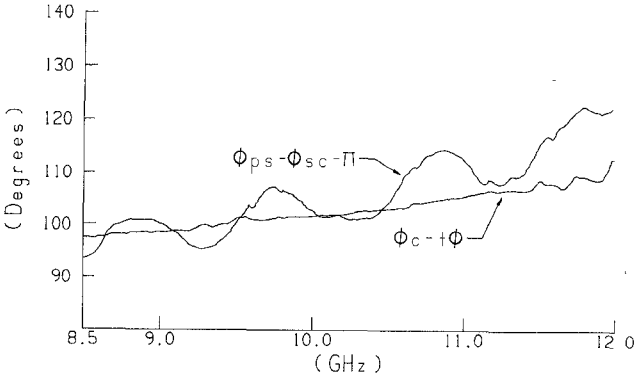

Fig. 6. Phase response of phase shifting networks.

Fig. 6 shows $\phi_{ps} - \phi_{sc} - \pi$ and $\phi_c - \phi_t$. Agreement is generally within 10° and this is considered acceptable bearing in mind the use of flexible guide. The ripple was present in ϕ_{sc} only and is probably due to finite isolation and mismatches in the coupler.

It is the use of this phase shifting network in the six-port circuit which allows for performance independent of phase velocity inequalities in the couplers and transmission line. This is because every wave contributing to a given detector response passes through the same number of couplers. For example, considering detector 3 the incident wave reflected from the short circuit passes through five couplers (two through paths and three coupled paths). The other incident wave passes through five couplers as well when the coupler-based phase shifting network is used since the phase shifting path consists of a coupled and a through path.

VI. Dielectric Waveguide Assembly for W-Band

Various considerations govern the choice of dielectric material to be used as the waveguide. A low dielectric constant is necessary to achieve broad-band operation with minimum dispersion [2]. For a given upper frequency of monomode operation this also allows the use of larger cross-sectional guide dimensions. Relative permittivities of approximately 2 allow waveguide band coverage with the dielectric guide cross section matching that of rectangular waveguide. This is desirable because power is normally launched onto the dielectric guide via rectangular waveguide transitions and the latter can thus provide rigid support for the dielectric.

Cross-linked polystyrene, $\epsilon_r = 2.54$, was chosen as the dielectric for the above reasons and furthermore is low loss, $\tan\delta = 0.0003$, and easy to machine. The cross-sectional dimensions chosen were 2.54 mm $\times$ 1.27 mm, which matched those of W-band rectangular waveguide. Transitions at each of the six-ports to detectors, source, and DUT were via 20 dB gain horns [25] with a 20 mm extra length of rectangular waveguide. The dielectric formed a close fit for 4 mm into the rectangular waveguide and was then uniformly tapered to a point, in both the horizontal and vertical planes, over a length of 15 mm.

Choice of quadrature hybrids will determine the bandwidth of the six-port reflectometer. Distributed hybrid couplers [26], [27] in dielectric-type waveguide tend to be narrow-band because they employ evanescent field interaction, which is strongly frequency dependent. It has been shown that the dielectric film coupler [24] exhibits broadband performance, and further work [23] has verified its quadrature action. It was therefore used both as the quadrature coupler and in realizing the phase shifting network. True 3 dB performance requires a film with $\epsilon_r = 6.78$ and 0.362 mm thickness for the given guide parameters. As this relative dielectric constant was not available, Stycast HiK, $\epsilon_r = 6$, with thickness 0.38 mm was used, giving a theoretical 3.5 dB coupling at 95 GHz with 0.5 dB maximum variation at 75 GHz and 110 GHz. Lastly the short circuit was constructed by first depositing a thin layer, 0.05 μm, of chrome on a 2.5 cm $\times$ 2.5 cm glass slide and over the chrome a 2 μm layer of gold. Two short circuits were also used as reflectors in the phase shifting network. Recalling that the coupled and through ports need to be connected together, then two options avail themselves. Firstly, a curved section of dielectric waveguide can be used which must adhere to a minimum bend radius [28] to avoid radiation losses. Alternatively, a straight section of guide can connect the coupled and through ports with reflectors to alter the propagation direction. Since two reflectors are used, an extra 360° phase shift is introduced, which does not affect the phase shifting properties of the network.

In order to minimize losses due to connections within the circuit butt joints were kept to a minimum by constructing the circuit out of four sections of dielectric guide. Each section was supported by at least one transition and further support was provided by an expanded polystyrene base which had negligible effect on propagation. The completed assembly was housed in an aluminum box with absorber lining the interior surfaces so as to reduce the effect of any internal stray radiation. Fig. 7 shows a photograph of the six-port circuit.

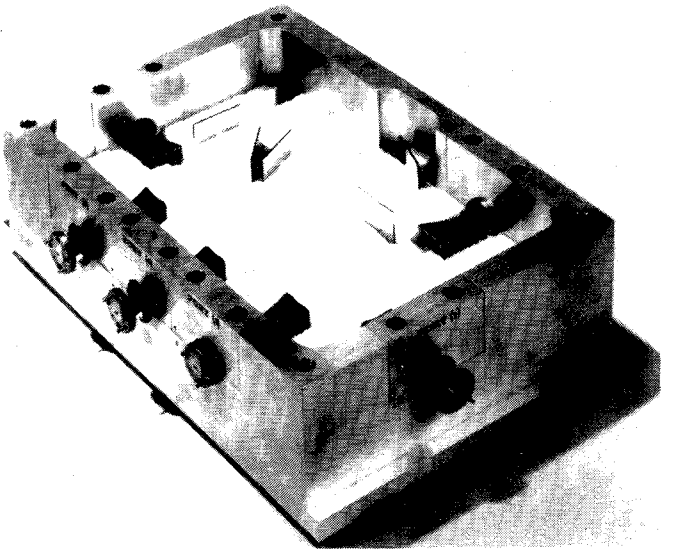

Fig. 7. W-band dielectric guide six-port reflectometer.

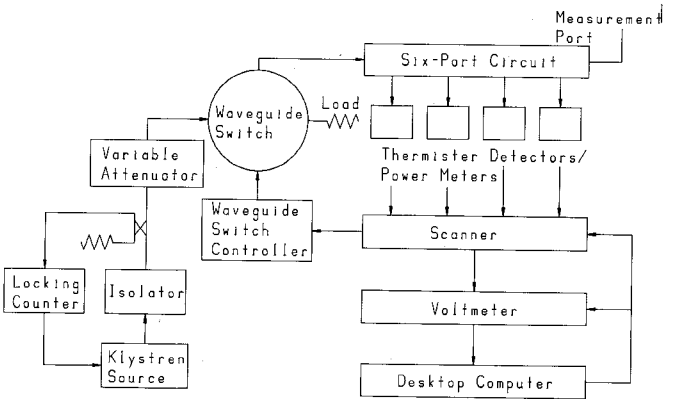

Fig. 8. Calibration and measurement setup.

VII. Calibration and Measurements

The calibration of the six-port circuit and subsequent measurements were carried out using a setup at R.S.R.E. Malvern, U.K., a schematic of which is shown in Fig. 8. The six- to four-port reduction calibration routine [29], [30] was employed as this requires a minimum number of standards. Ten loads were used for calibration, of which three were accurately known standards and were realized by offsetting a short circuit from the measurement plane with the aid of rectangular waveguide spacers. A nominally matched load provided the half standard for resolving the sign ambiguity [30] encountered in the six- to four-port reduction. For the rest, a movable short circuit was preceded by a variable attenuator, and altering the settings enabled the other six loads to be realized. The data from all ten loads were used in the reduction while those from the standards enabled the equivalent four-port to be calibrated.

Calibration was attempted between 77 and 105 GHz inclusive and the iterative solution for the reduction constants generally converged to six decimal places within five iterations.

The positions of the impedance locating circle centers can be evaluated for different loads [30] and these are shown in Table I at 80 GHz. It can be seen that the variation is small and this is a consequence of good coupler isolation and detector match. Similar behavior was obtained at all calibration frequencies. Fig. 9 shows the positions of the impedance locating circle centers for the

TABLE I
VARIATION OF CIRCLE CENTERS WITH LOAD AT 80 GHz

Voltage Reflection Coefficient of Load		Positions of Circle Centres in the Γ Plane					
		Centre A		Centre B		Centre C	
Real	Imaginary	Real	Imaginary	Real	Imaginary	Real	Imaginary
0.669160	0.743118	-1.013	1.475	-0.844	-2.561	1.062	-0.421
0.764543	-0.644572	-0.984	1.531	-0.703	-2.483	0.998	-0.385
-0.612159	-0.790735	-0.896	1.607	-0.588	-2.366	0.993	-0.370
-0.010632	-0.003894	-0.856	1.646	-0.539	-2.308	0.971	-0.328
-0.104441	-0.058846	-0.886	1.653	-0.533	-2.314	0.967	-0.287
-0.242686	0.113098	-0.874	1.638	-0.548	-2.331	0.961	-0.264
-0.477357	0.369087	-0.842	1.633	-0.552	-2.319	0.983	-0.345
-0.111634	0.675536	-0.861	1.640	-0.541	-2.280	0.995	-0.393
0.526505	0.743981	-0.873	1.635	-0.595	-2.357	0.999	-0.407
0.908033	-0.037462	-0.893	1.610	-0.598	-2.360	1.112	-0.413

TABLE II
MEASUREMENTS OF OFFSET SHORT CIRCUITS

Frequency	Calculated Reflection Coefficient of Load		Measured Reflection Coefficient		Standard Deviation	
	Magnitude	Phase (degrees)	Magnitude	Phase (degrees)	Magnitude	Phase (degrees)
77	1.00000	59.115	0.99805	58.917	0.00037	0.019
	1.00000	- 21.594	0.99765	- 21.106	0.00019	0.038
	1.00000	-142.836	1.00088	-143.164	0.00056	0.061
94	1.00000	1.212	0.99628	1.417	0.00076	0.239
	1.00000	-118.155	0.99510	-118.863	0.00246	0.078
	1.00000	123.180	0.99276	123.555	0.00492	0.144
100	1.00000	- 17.264	0.99878	- 17.729	0.00078	0.103
	1.00000	-148.966	1.00287	-148.371	0.00266	0.331
	1.00000	80.106	1.00354	79.443	0.00041	0.244

matched load case at some of the calibration frequencies together with those predicted for 3 dB couplers.

Table II shows measurements made on offset short circuits, different from those used in calibration, at representative frequencies. The measured value is an average one taken over five consecutive measurements, which allows a standard deviation to be calculated. The latter may be thought of as an indication of the effect of noise, in the detectors and data acquisition, on measurement. It can be seen that the differences between measured and calculated values cannot be accounted for by noise alone. This is in part due to the finite loss in the spacers, used to offset the short circuit, not being incorporated into the calculated value. However, the measurement accuracy is generally within 0.5 percent in magnitude and 0.7° in phase for $|\Gamma| = 1$ loads.

VIII. CONCLUSIONS

This paper describes the design and performance of a six-port reflectometer circuit implemented in *W*-band dielectric waveguide. The design used three 3 dB broad-band quadrature couplers which were specific to dielectric wave-

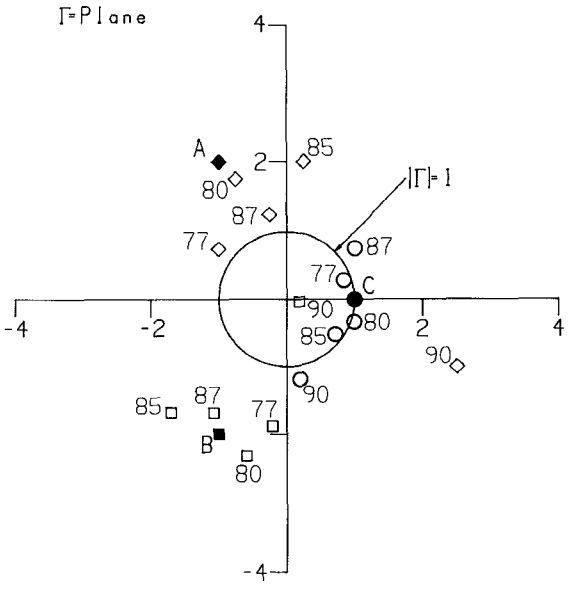

Fig. 9 Positions of circle centers in the Γ plane.

guide as well as a novel broad-band phase shifting network. The overall dimensions were fixed by the size of the external power sensors; in practice this could have been reduced much further with integrated sensors.

Ideal couplers and matched sensors were assumed in the analysis so that the design process could be simplified. This approach was subsequently justified by the experimental results of Table I, where the circle centers do not have a large variation with DUT.

The performance of the six-port reflectometer has been demonstrated at various frequencies in the range 75–105 GHz. The accuracy of the measurements on various short circuits was within 0.5 percent in amplitude and 0.7° in phase. The complete results are shown in Table II.

This paper shows that this six-port circuit can be used with dielectric waveguide over a complete metallic rectangular waveguide bandwidth (75–110 GHz). The authors have also implemented this circuit successfully in the following bands and transmission lines:

26–40	GHz in image guide and rectangular waveguide
2–18	GHz in triplate and coaxial guide
8.5–12	GHz in rectangular waveguide
10–200	MHz in coaxial lumped components

The circuit configuration is sufficiently simple to be implemented in any transmission line which is suitable for the frequency range.

References

[1] R. J. Collier and P. D. White, "Attenuation measurement of dielectric guide," *Electron. Lett.*, vol. 10, nos. 25/26, p. 526, Dec. 1974

[2] R. J. Collier and R. D. Birch, "The bandwidth of image guide," *IEEE Trans. Microwave Theory Tech.*, vol. MTT-28, pp. 932–935, Aug. 1980.

[3] R. M. Knox and P. P. Toulios, "Integrated circuits for the millimeter through optical frequency range," in *Proc. Symp. Submillimeter Waves*, Polytechnic Press of Polytechnic Institute of Brooklyn, Brooklyn, NY, 1970, pp. 497–516.

[4] T. Yoneyama and S. Nishida, "Nonradiative dielectric waveguide for millimeter-wave integrated circuits," *IEEE Trans. Microwave Theory Tech.*, vol. MTT-29, Nov. 1981.

[5] T. Itok and F. J. Hsu, "Distributed Bragg reflector gun oscillator for dielectric millimetre-wave integrated circuits," in 1980 *IEEE MTT-S Int. Microwave Symp. Dig.*, May 1980, pp. 205–207.

[6] E. A. J. Marcatili, "Dielectric rectangular waveguide and directional coupler for integrated optics," *Bell Syst. Tech. J.*, vol. 48, no. 7, pp. 2079–2102, Sept. 1969.

[7] J. E. Goell, "A circular-harmonic computer analysis of rectangular dielectric waveguides," *Bell Syst. Tech. J.*, vol. 48, no. 7, pp. 2133–2160, Sept. 1969.

[8] K. Solback and I. Wolff, "The electromagnetic fields and the phase constants of dielectric image lines," *IEEE Trans. Microwave Theory Tech.*, vol. MTT-26, pp. 266–274, Apr. 1978.

[9] B. M. Azizur and J. B. Davies, "Finite element analysis of optical and microwave waveguide problems," *IEEE Trans. Microwave Theory Tech.*, vol. MTT-32, pp. 20–28, Jan. 1984.

[10] R. Rudokas and T. Itoh, "Passive millimetre-wave I.C. components made of inverted strip dielectric waveguide," *IEEE Trans. Microwave Theory Tech.*, vol. MTT-24, pp. 978–981, Dec. 1976.

[11] M. J. Aylward and N. Williams, "Low cost millimeter wave transmission lines and components," ERA Technology Ltd., Report No. RFTC150176, Annual Report 1977.

[12] R. D. Birch, "Image guide," Ph.D. Thesis, University of Kent at Canterbury, U.K., 1981.

[13] C. A. Hoer, "The six-port coupler: A new approach to measuring voltage current, power impedance and phase," *IEEE Trans. Instrum. Meas.*, vol. IM-21, pp. 466–470, Nov. 1972.

[14] G. F. Engen and C. A. Hoer, "Application of an arbitrary 6-port junction to power-measurement problems," *IEEE Trans Instrum. Meas.*, vol. IM-21, pp. 470–474, Nov. 1972.

[15] G. F. Engen, "The six-port reflectometer: An alternative network analyser," *IEEE Trans. Microwave Theory Tech.*, vol. MTT-25, pp. 1075–1080, Dec. 1977.

[16] R. A. Hackborn, "An automatic network analyser system," *Microwave J.*, vol. 11, pp. 45–52, May 1968.

[17] G. F. Engen and R. W. Beatty, "Microwave reflectometer techniques," *IRE Trans. Microwave Theory Tech.*, vol. MTT-7, pp. 351–355, 1959.

[18] J. A. Dobrowolski, "Improved six-port circuit for complex reflection coefficient measurements," *Electron. Lett.*, vol. 18, pp. 748–750, Aug. 1980.

[19] G. P. Riblet, "A compact waveguide 'resolver' for the accurate measurement of complex reflection and transmission coefficients using the 6-port measurement concept," *IEEE Trans. Microwave Theory Tech.*, vol. MTT-29, p. 155–162, Feb. 1981.

[20] G. F. Engen, "An improved circuit for implementing the six-port technique of microwave measurements," *IEEE Trans. Microwave Theory Tech.*, vol. MTT-25, pp. 1080–1083, Dec. 1977.

[21] E. J. Griffin, G. J. Slack, and L. D. Hill, "Broadband six-port reflectometer junction," *Electron. Lett.*, vol. 19, pp. 921–922, Oct. 1983.

[22] R. J. Collier, G. Hjipieris, and E. J. Griffin, "Six-port reflectometer," Patent 8413339.

[23] G. Hjipieris, "Millimetre wave six-port reflectometry using image and dielectric guides," Ph.D. thesis, University of Kent at Canterbury, U.K., 1985.

[24] R. J. Collier and G. Hjipieris, "A broad-band directional coupler for both dielectric and image guides," *IEEE Trans. Microwave Theory Tech.*, vol. MTT-33, Feb. 1985.

[25] T. N. Trink, J. AG. Malherbe, and R. Mittra, "A metal-to-dielectric waveguide transition with applications to millimetre-wave integrated circuits," in 1980 *IEEE MTT-5 Int. Microwave Symp. Dig.*, May 1980, pp. 205–207.

[26] K. Solbach, "The calculation and the measurement of the coupling properties of dielectric image lines of rectangular cross section," *IEEE Trans. Microwave Theory Tech.*, vol. MTT-27, pp. 54–58, Jan. 1979.

[27] J. A. Paul and P. C. H. Yen, "Millimetre-wave passive components and six-port network analyser in dielectric waveguide," *IEEE Trans. Microwave Theory Tech.*, vol. MTT-29, pp. 948–953, Sept. 1981.

[28] E. A. J. Marcatili and S. E. Miller, "Improved relations describing directional control in electromagnetic wave guidance," *Bell Sys. Tech. J.*, vol. 48, no. 7, pp. 2161–2188, Sept. 1969.
[29] G. F. Engen, "Calibrating the six-port reflectometer by means of sliding terminations," *IEEE Trans. Microwave Theory Tech.*, vol. MTT-26, pp. 951–957, Dec. 1978.
[30] T. E. Hodgetts and E. J. Griffin, "A unified treatment of the theory of six-port reflectometer calibration using the minimum of standards," R.S.R.E. Report No. 83003.

✠

George Hjipieris (M'87) was born in Melbourne, Australia, in 1958. He received the B.Sc. (Hons) and Ph.D. degrees in electronics in 1981 and 1984 respectively from the University of Kent, Canterbury, England.

In 1984 he joined Marconi Instruments, Stevenage, England, where he now heads the Microwave Components Group. His main interests are microwave measurement techniques, broad-band component design, and microwave systems.

Richard J. Collier was born in Leicester, England, in 1940. He gained B.Sc. (Hons) and Ph.D. degrees at the University of Southampton in 1963 and 1966 respectively.

After three years as a research fellow at the National Physical Laboratory he joined the academic staff at the University of Kent, Canterbury, England. He is now a Senior Lecturer in Electronic Engineering and his research interests include microwave measurements and medical electronics.

✠

Eric J. Griffin started working on microwave standards in 1966 at S.E.S.C. Harefield and later moved to R.S.R.E. Malvern in 1968. Since then he has specialized in six-port and multiport reflectometers. He was the founding chairman of the Automated Radio and Microwave Measurement Society (ARMMS) in the U.K.